Sarcolemmal ion currents and sarcoplasmic reticulum Ca²⁺ content in ventricular myocytes from the cold stenothermic fish, the burbot (*Lota lota*)

Holly A. Shiels[1],[*], Vesa Paajanen[2] and Matti Vornanen[2]

[1]*Faculty of Life Sciences, University of Manchester, 2.18c Core Technology Facility, 46 Grafton Street, Manchester, M13 9NT, UK and* [2]*Department of Biology, University of Joensuu, PO Box 11, 80101 Joensuu, Finland*

[*]Author for correspondence (e-mail: holly.shiels@manchester.ac.uk)

Summary

The burbot (*Lota lota*) is a cold stenothermic fish species whose heart is adapted to function in the cold. In this study we use whole-cell voltage-clamp techniques to characterize the electrophysiological properties of burbot ventricular myocytes and to test the hypothesis that changes in membrane currents and intracellular Ca²⁺ cycling associated cold-acclimation in other fish species are routine for stenothermic cold-adapted species. Experiments were performed at 4°C, which is the body temperature of burbot for most of the year, and after myocytes were acutely warmed to 11°C, which is in the upper range of temperatures experienced by burbot in nature. Results on K⁺ channels support our hypothesis as the relative density of K-channel conductances in the burbot heart are similar to those found for cold-acclimated cold-active fish species. I_{K1} conductance was small (39.2±5.4 pS pF⁻¹ at 4°C and 71.4±1.7 pS pF⁻¹ at 11°C) and I_{Kr} was large (199±27 pS pF⁻¹ at 4°C and 320.3±8 pS pF⁻¹ at 11°C) in burbot ventricular myocytes. We found high Na⁺–Ca²⁺ exchange (NCX) activity (35.9±6.3 pS pF⁻¹ at 4°C and 58.6±8.4 pS pF⁻¹ at 11°C between –40 and 20 mV), suggesting that it may be the primary pathway for sarcolemmal (SL) Ca²⁺ influx in this species. In contrast, the density (I_{Ca}, 0.81±0.13 pA pF⁻¹ at 4°C, and 1.35±0.18 pA pF⁻¹ at 11°C) and the charge (Q_{Ca}, 0.24±0.043 pC pF⁻¹ at 4°C and 0.21±0.034 pC pF⁻¹ at 11°C) carried by the L-type Ca²⁺ current was small. Our results on sarcolemmal ion currents in burbot ventricular myocytes suggest that cold stenothermy and compensative cold-acclimation involve many of the same subcellular adaptations that culminate in enhanced excitability in the cold.

Key words: action potential, Na⁺–Ca²⁺ exchange, L-type Ca²⁺ channel, K⁺ channel, I_{Ca}, I_{Kr}, I_{K1}, sarcoplasmic reticulum (SR), temperature, fish heart, caffeine, isoprenaline, burbot, *Lota lota*.

Introduction

Ectotherms are able to acclimatize to different temperatures, adjusting physiological and biochemical processes to meet the demands of their environment. Acclimatization of the heart is especially important as cardiac output must match the changes in activity level, metabolic rate and blood viscosity that occur with changes in temperature. The effects of temperature acclimation on cardiac contractility in ectotherms are well documented (Keen et al., 1994; Shiels and Farrell, 1997; Aho and Vornanen, 1999) (for a review, see Driedzic and Gesser, 1994). More recent work has focused on elucidating adaptations in cardiac myocyte excitability (Vornanen et al., 2002a; Paajanen and Vornanen, 2004), cellular Ca²⁺ cycling (Hove-Madsen and Tort, 1998; Hove-Madsen et al., 1998; Harwood et al., 2000, Shiels et al., 2000; Shiels et al., 2002a; Shiels et al., 2002b; Hove-Madsen et al., 2003) and protein structure (Yang et al., 2000; Gillis et al., 2000; Gillis et al., 2003) associated with maintained cardiac viability in the cold (for reviews, see Vornanen et al., 2002b; Gillis and Tibbits,

2002). Although some ectotherms cope with cold temperatures *via* cold-torpor and resultant reductions in metabolic rate and heart rate, there are several compensatory changes often associated with ectotherms that remain active in the cold. These include an increase in relative ventricular mass, possibly to offset increased blood viscosity (Goolish, 1987; Graham and Farrell, 1989), a proliferation of the sarcoplasmic reticulum (SR) (Bowler and Tirri, 1990) suggesting increased reliance on intracellular Ca²⁺ cycling during excitation–contraction coupling (Keen et al., 1994; Shiels and Farrell, 1997; Aho and Vornanen, 1999; Tiitu and Vornanen, 2002b) and changes in K⁺ channel conductances that decrease action potential duration (APD) ensuring myocyte excitability in the cold (Vornanen et al., 2002a; Paajanen and Vornanen, 2004).

Some ectothermic animals do not tolerate large seasonal increases in temperature, and therefore inhabit a cold stenothermic environment. Fish species such as the burbot *Lota lota*, are cold stenotherms spending most of their life at temperatures between 1°C and 7°C, and are rarely found in

waters above 13°C (Carl, 1995). Burbot are benthic, and are sluggish swimmers but are cold-active, spawning in winter under ice-covered lakes (Pääkkönen and Marjomäki, 2000). Examination of burbot heart morphology and contractility suggests that the changes normally associated with cold-acclimation in active species such as rainbow trout (*Oncorhynchus mykiss*), may be routine for cold-adapted species. The relative ventricular mass of the burbot (~0.15% body mass) is elevated in comparison with most eurythermal species (~0.08% body mass) (Tiitu and Vornanen, 2002a). Both atrial and ventricular muscle isolated from burbot heart exhibit increased ryanodine-sensitivity of contraction, suggesting that the SR may be routinely involved in delivering Ca^{2+} to the myofilaments during force development (Tiitu and Vornanen, 2002b). Furthermore, [^{3}H]ryanodine binding to cardiac preparations from burbot and rat show similar Ca^{2+}-dependent activation of the SR Ca^{2+} release channel, suggesting that Ca^{2+}-induced Ca^{2+}-release (CICR) may operate during excitation–contraction coupling in this species (Vornanen, 2006). Collectively, these results suggest that many of the subcellular changes that are required to maintain cardiac function during cold acclimation may also play a role in long-term cold adaptation. However, at present no studies have examined excitation–contraction coupling at the level of the myocyte in the burbot or any cold stenothermic species.

In this study, we investigated the electrophysiological properties of burbot ventricular myocytes at 4°C, which is the typical habitat temperature of this species for most of the year. We also examined electrophysiological parameters after acutely warming the myocytes to 11°C because we were interested in how excitation–contraction coupling in the stenothermic heart is modulated during acute temperature change and because 11°C is approaching the upper temperature at which this species is found (Carl, 1995; Pääkkönen and Marjomäki, 2000). We first set out to measure APs and the major sarcolemmal (SL) ion currents involved in regulating myocyte excitability and maintaining electrical stability in the cold. Next, to investigate possible changes in cellular Ca^{2+} dynamics in a cold-adapted species we examined SR Ca^{2+} accumulation and release using caffeine. We assumed that if the changes found in rainbow trout and other active teleosts under cold-acclimation were adaptive, then, through evolutionary processes, similar changes may be permanent in the genome of cold stenothermic fish. First, we hypothesized that reorganisation of K^+ currents would occur with a shift from the dominance of the inward rectifier K current (I_{K1}) in favour of the delayed rectifier K^+ current (I_{Kr}) (Vornanen et al., 2002a). Second, we expected that intracellular Ca^{2+} stores of the SR would make a significant contribution to excitation–contraction coupling (Tiitu and Vornanen, 2002b) and appear as accelerated decay of the L-type Ca^{2+} current (I_{Ca}) (Shiels et al., 2002b). In agreement with the first hypothesis, I_{K1} was small and I_{Kr} large in ventricular myocytes of the burbot heart. However, we did not find evidence of increased SR Ca^{2+} involvement in our measurements of I_{Ca} inactivation.

Rather, we report an increase in SL Na^+–Ca^{2+} exchange (NCX) activity, which we suggest is the primary pathway for SL Ca^{2+} influx in this species.

Materials and methods
Fish origin and care

Sexually mature burbot *Lota lota* L. (body mass 224.6±12.7 g, *N*=22) of both sexes were caught during spawning time from Lake Orivesi (62°30′N) in Finland. In the laboratory fish were held in 500 liter stainless steel tanks at 4°C with continuous circulation (approximately 0.5 l min^{-1}) of aerated groundwater. Fish were fed with dead vendace (*Coregonus albula*) three times a week. Photoperiod was 15 h:9 h dark:light.

Myocyte isolation

All procedures were in accordance with local animal handling protocols. A detailed description of myocyte preparation has been previously published for other fish species (Vornanen, 1997; Shiels et al., 2000). Briefly, fish were stunned with a blow to the head, the spine was cut just behind the brain and the heart was excised. The heart was then perfused first with an isolating solution for 8–10 min, and then with a proteolytic enzyme solution for 15 min at ~15°C. After enzymatic treatment, the ventricle was placed in isolating solution, cut into small pieces with scissors and then triturated through the opening of a Pasteur pipette to free individual myocytes. The myocytes were stored in fresh isolating solution at 4°C and used within 8 h.

Solutions

The isolating solution contained (mmol l^{-1}): NaCl 100, KCl 10, KH_2PO_4 1.2, $MgSO_4$ 4, taurine 50, glucose 20, and Hepes 10, adjusted to pH 6.9 with KOH. For enzymatic digestion, collagenase (Type IA from Sigma, St Louis, MI, USA; 0.75 mg ml^{-1}), trypsin (Type IX from Sigma; 0.5 mg ml^{-1}) and fatty acid-free bovine serum albumin (BSA, from Sigma; 0.75 mg ml^{-1}) were added to this solution.

The external solution used for measuring ventricular action potentials (AP) contained (mmol l^{-1}): NaCl 150, KCl 3, $MgSO_4$ 1.2, NaH_2PO_4 1.2, $CaCl_2$ 1.8, glucose 10 and Hepes 10, adjusted to pH 7.6 with NaOH. The external solution used for measuring K^+ currents contained (mmol l^{-1}): NaCl 150, KCl 5.4, $CaCl_2$ 1.8, $MgCl_2$ 1.2, glucose 10 and Hepes 10, adjusted to pH 7.6 with NaOH at 20°C. Specific inhibition of the rapid component of the delayed rectifier K^+ current (I_{Kr}) was accomplished with E-4031 (1 μmol l^{-1}; Alomone Labs Ltd, Jerusalem, Israel). The external solution used for measuring Na^+–Ca^{2+} exchange current (I_{NCX}) and L-type Ca^{2+} current (I_{Ca}) contained (mmol l^{-1}): NaCl 150, CsCl 5.4, $MgSO_4$ 1.5, NaH_2PO_4 0.4, $CaCl_2$ 1.8, glucose 10 and Hepes 10, adjusted to pH 7.6 with CsOH. Unless otherwise stated, 0.5 μmol l^{-1} TTX (Tocris Cookson, Bristol, UK), 10 μmol l^{-1} nifedipine and 100 μmol l^{-1} ouabain (both from Sigma) were included to block Na^+ channels, L-type Ca^{2+} channels and Na^+/K^+ ATPase,

respectively, when recording I_{NCX}. Nifedipine and ouabain were omitted when recording I_{Ca}.

The pipette solution used during K$^+$ current experiments contained (mmol l^{-1}): KCl 140, MgATP 4, MgCl$_2$ 1, EGTA 5 and Hepes 10, adjusted to pH 7.2 with KOH. Pipette solutions for measurement of I_{NCX} contained (mmol l^{-1}): CsCl 140, MgCl$_2$ 1, CaCl$_2$ 9, BAPTA 20, Na$_2$ATP 5, Na$_2$GTP 0.03 and Hepes 10, adjusted to pH 7.2 with CsOH at 20°C. The free intracellular Ca^{2+} concentration of this solution was calculated (MaxChelator) to be 179.5 and 186.6 nmol l^{-1} at 4° and 11°C, respectively. Under these conditions, intracellular calcium is buffered to a diastolic level. In some experiments, we investigated the effect of using a lower level of Ca^{2+} buffering on I_{NCX} by replacing BAPTA with 0.025 mmol l^{-1} EGTA. I_{Ca} was initially characterised with pipettes containing (mmol l^{-1}): CsCl 130, MgATP 5, tetraethylammonium chloride (TEA) 15, MgCl$_2$ 1, oxaloacetate 5, EGTA 5, Na$_2$GTP 0.03 and Hepes 10 adjusted to pH 7.2 with CsOH. In latter experiments I_{Ca} and SR Ca^{2+} loading were assessed using the same pipette solution except that EGTA concentration was decreased from 5 mmol l^{-1} to 0.025 mmol l^{-1} to better mimic *in vivo* cytosol Ca^{2+} buffering (Hove-Madsen and Tort, 1998). Steady-state kinetics parameters of I_{Ca} were obtained by fitting activation and inactivation data to Boltzman functions to determine the half-activating, half-inactivating potentials (V_h) and the slope (k) of activation and inactivation, as previously described (Vornanen, 1998).

Experimental procedures

Intracellular APs were measured from spontaneously beating whole-heart preparations at 4°C and 11°C as described previously (Vornanen, 1996). Briefly, the excised ventricle was medially opened, spread and secured on the bottom of a 10 ml tissue chamber filled with oxygenated saline. Ventricular APs were recorded using high-resistance microelectrodes (30–60 MΩ when filled with 3 mol l^{-1} KCl) fabricated from borosilicate glass (World Precision Instruments, 1BBL, Sarasota, FL, USA) with a two-stage horizontal puller (Campden Instruments Ltd, UK). Microelectrode signals were recorded using a high-impedance amplifier (KS-700, WPI, Sarasota, FL, USA), digitized (DigiData 1200, Axon Instruments, Foster City, CA, USA) and stored to a computer using Axotape 2.2 acquisition software and then analysed off-line (Clampfit, Axon Instruments). The time course of contraction was recorded simultaneously with APs by attaching one corner of the ventricle to a force transducer (FT03 Grass Instruments, West Warwick, RI, USA) by a small metal hook and braided silk thread. Muscle was slightly tensioned and the force signal was amplified by a Grass 7D polygraph amplifier and fed through the digitizer to the computer for later off-line analysis.

Stimulation, acquisition and analysis of ventricular myocyte whole-cell voltage and current signals was achieved using established methods (Vornanen, 1997; Shiels et al., 2000; Paajanen and Vornanen, 2002) on either an Axopatch 1D amplifier in conjunction with pClamp 8.2 and Clampfit

software, or on an EPC-9 amplifier in conjunction with Pulse 6.3 and Pulsefit software (Heka, Lambrecht, Germany). Myocytes (capacitance 23.7±0.5 pF, N=179 cells) were placed in the recording chamber (RCP-10T, Dagan, Maryland, MI, USA, volume 500 μl or RC-26, Warner Instruments Corp. Brunswick, Handen, CT, USA, volume 150 μl) and were superfused continuously with external saline at the rate of 1.5–2 ml min^{-1}. The temperature of the saline was regulated at either 4±1°C or 11±1°C by circulating water baths or a Peltier device. Bath temperature was continuously monitored by thermocouples positioned no less than 5 mm from the cell under investigation. Patch electrodes were pulled from borosilicate glass (Garner F-78045, Claremont, CA, USA) with a two-stage vertical puller (L/M-3P-A, List Medical, Darmstadt, Germany). The resistance of the electrodes was 2–4 MΩ when filled with pipette solutions. Pipette and whole cell capacitances were routinely compensated, and access resistance was recorded but not compensated. Currents were filtered at 2.0 kHz using either a 4-pole or a 8-pole Bessel filter.

During SR Ca^{2+} loading and release experiments, rapid (~50 ms) application of caffeine and/or channel inhibitors was achieved by switching between temperature controlled barrels of a rapid solution changer (RS200, Biologic, Claix, France). CdCl$_2$ (100 μmol l^{-1}) or a combination of CdCl$_2$ (30 μmol l^{-1}) and verapamil (10 μmol l^{-1}) was used to rapidly block I_{Ca}. NiCl$_2$ (10 mmol l^{-1}) was used to inhibit the NCX. SR Ca^{2+} content was assessed by the application of caffeine (10 mmol l^{-1}), which induces the release of Ca^{2+} from the SR. This Ca^{2+} is then extruded from the cell *via* the NCX generating an inward current (see Results), which is directly proportional to the Ca^{2+} released from the SR (Varro et al., 1993). The time integral of this caffeine-induced I_{NCX} current was used to calculate the SR Ca^{2+} content (in pC) at the time of caffeine application. This value was expressed per unit capacitance (pC pF^{-1}). SR Ca^{2+} content was also expressed in μmol Ca^{2+} l^{-1} non-myofibrillar cell volume [40% as determined previously (Vornanen, 1998)]. Cell volume was calculated from cell surface area, obtained by measurements of cell capacitance (pF) and assuming a specific membrane capacitance of 1.59 μF cm^{-2}, and a surface-to-volume ratio of 1.15.

Details of the voltage clamp waveforms and protocols used to study the electrophysiological properties of whole-cell currents are provided in the results and the figures. When values are presented as means, the number of observations (N) and statistical significance are provided in the text or appropriate figure legend.

Results

Action potential characteristics in burbot ventricular myocytes

At 4°C the beating frequency of the burbot heart was 17.98±0.36 contractions min^{-1} (N=10) (0.3 Hz). The duration of contraction and AP closely matched and were slightly less than 2 s at 4°C (Fig. 1). The close match between AP duration (APD) and the duration of contraction suggest that the
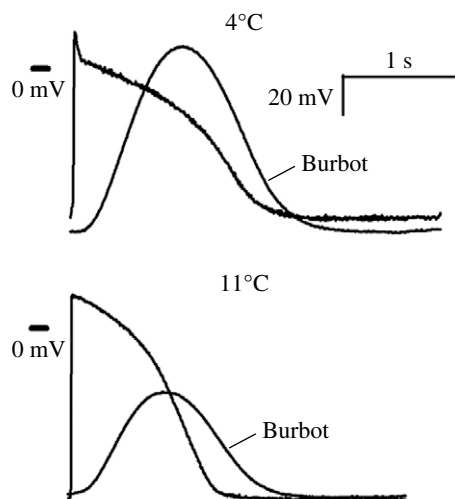
Fig. 1. Representative recordings of ventricular action potentials and associated contractions of the burbot ventricle at 4°C and 11°C. Scale bars are for recordings at both temperatures. Force of contraction is in arbitrary units.

activation and relaxation of cardiac twitch are governed by membrane potential. Peak ventricular force occurred when the AP had repolarised to about –20 mV. The resting membrane potential (RMP) and AP overshoot were –70.4±1.1 mV and 14.4±0.7 mV, respectively (N=10). AP duration at plateau (0 mV), and at 50, 90 and 100% repolarisation was 292±48, 1108±28, 1544±29 and 1830±46 ms, respectively (N=10). At 11°C, RMP and AP overshoot were –75.0±1.8 and 15.8±1.2 mV, respectively, whereas corresponding values of AP duration were 250±44, 771±39, 1159±61 and 1313±72 ms at 0 mV, and at 50, 90 and 100% repolarisation, respectively (N=12). The APD was significantly shorter at 11°C than 4°C with APD at 90% repolarization (APD_{90}) values of 1091±179 and 1594±16 ms, respectively (P<0.0002). Absolute force decreases with increasing temperature (Fig. 1). This was a regular finding and has been quantitatively reported previously (see Tiitu and Vornanen, 2002b).

K^+ currents in burbot ventricular myocytes

The two main K^+ currents in burbot ventricular myocytes are the background inward rectifier (I_{K1}) and the rapid component of the delayed rectifier current (I_{Kr}). The conductance of I_{K1}, which is the major K^+ current in ventricular myocytes of most vertebrate species, was surprisingly low in burbot myocytes (39.2±5.4 pS pF^{-1} at 4°C; Fig. 2A). Even at 11°C, I_{K1} conductance of the burbot ventricular myocyte was only 71.4±1.7 pS pF^{-1}. In contrast, the size of I_{Kr} was large. At 4°C, the maximum density of the E4031-sensitive (1 μmol l^{-1}) tail current was 2.9±0.3 pA pF^{-1} (Fig. 2B). When temperature was increased to 11°C, current density increased to 3.8±1.1 pA pF^{-1} (P=0.04) and caused a 15 mV shift (P=0.04) of the current–voltage relation to hyperpolarising voltages. The slope conductance of I_{Kr} was 199±27 and 320±8 pS pF^{-1} at 4°C and 11°C, respectively, i.e. 4.5–5 times that of the I_{K1}.
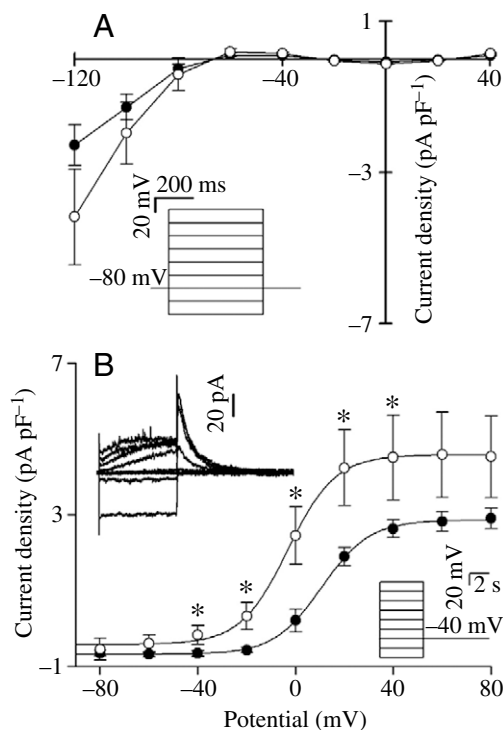

Fig. 2. The two major K^+ currents in burbot ventricular myocytes. (A) Background inward rectifier K^+ current, I_{K1}. Values are means ± s.e.m. from 6–8 cells at 4°C (black circles) and 11°C (white circles) measured at the beginning of 500 ms square wave pulses that were elicited from the holding potential of –80 mV to voltages between –120 and 40 mV in 20 mV steps (inset). (B) Delayed rectifier K^+ current, I_{Kr}, measured as an outward tail current at –40 mV after 5 s depolarising pulses between –80 and 80 mV (inset). Representative recordings at 4°C and mean values (± s.e.m.) from 5–10 cells at 4°C (black circles) and 11°C (white circles). *Density of I_{Kr} is increased significantly by acute warming to 11°C (Student's t-test, P<0.005).

I_{NCX} in burbot ventricular myocytes

We investigated the efficacy of the NCX at two different levels of intracellular Ca^{2+} buffering. In the first series of experiments (Fig. 3A) we measured the NCX under conditions that held intracellular Ca^{2+} at diastolic levels (see Materials and methods). I_{NCX} was elicited at 4 s intervals from the calculated reversal potential of the exchanger (–26.5 mV) by ramp pulses (Fig. 3A, inset). I_{NCX} was measured as the Ni^{2+}-sensitive current during the hyperpolarizing phase of the ramp. At 4°C, the conductance of I_{NCX} was 35.9±6.3 pS pF^{-1} between –40 and 20 mV and it increased with a Q_{10} of 2.49±0.29 to 58.6±8.4 pS pF^{-1} when temperature was increased to 11°C (Fig. 3A). The measured reversal potential of I_{NCX} was –23.5±0.1 and –23.7±0.8 mV at 4°C and 11°C, respectively, which is close to theoretical equilibrium potential. Neither 2 μmol l^{-1} isoprenaline nor 10 mmol l^{-1} caffeine had any effect on burbot I_{NCX} (not shown). Isoprenaline (10 μmol l^{-1}) caused a small but non-significant (P=0.142, N=5) increase in I_{NCX} (not shown).

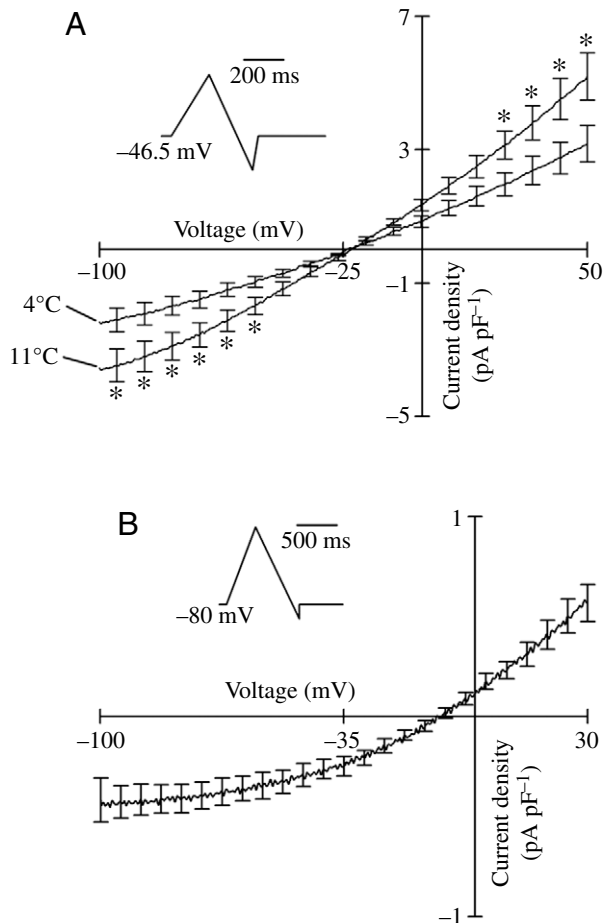In the second series of experiments we reduced intracellular

Fig. 3. Na$^+$–Ca^{2+} exchange current (I_{NCX}) measured as the Ni^{2+}-sensitive current during the hyperpolarising phase of the ramp pulse in ventricular myocytes from the burbot heart. (A) Values are means ± s.e.m. from 8 cells at 4°C and 11°C when the intracellular solution contained 20 mmol l^{-1} BAPTA. *Density of I_{NCX} is increased significantly by acute warming to 11°C (Student's *t*-test, $P<0.005$). (B) Mean values (± s.e.m.) from 9 cells at 4°C only. The pipette solution contained a lower level of Ca^{2+} buffering (0.025 mmol l^{-1} EGTA). Insets show voltage ramp protocols.

Ca^{2+} buffering to a more physiological level by replacing 20 mmol l^{-1} BAPTA with 0.025 mmol l^{-1} EGTA. Repolarising ramps from 30 to –100 mV were applied at every 4th second from a holding potential of –80 mV (see inset Fig. 3B). These experiments were preformed at 4°C only. The outward NCX current is significantly smaller in the weakly buffered pipette solution than in the heavily buffered solution given in Fig. 3A, with a mean conductance of 13.8±2.3 pS pF^{-1} at 10 mV. The mean reversal potential of the NCX current was –8.88±1.6 mV ($N=9$).

I_{Ca} in burbot ventricular myocytes

I_{Ca} was elicited from a holding potential of –80 mV to voltages between –70 and +60 mV for 1 s, in the absence and presence of a saturating concentration of isoprenaline (10 μmol l^{-1}) (Fig. 4). The density of I_{Ca} measured using 5 mmol l^{-1} EGTA, which will augment current amplitude, was only 0.81±0.13 pA pF^{-1} at 4°C, and increased to 1.35±0.18 pA pF^{-1} at 11°C (Q$_{10}$=2.08; P=0.01). The charge density (Q_{Ca}) of I_{Ca} was 0.24±0.043 pC pF^{-1} and 0.21±0.034 pC pF^{-1} at 4°C and 11°C, respectively. Temperature does not affect charge density (P=0.6), primarily due to the slowing of current decay at the colder temperature. Single exponential equations fit to the decay of the I_{Ca} under physiological buffering conditions (i.e. 25 μmol l^{-1} EGTA, Fig. 6C) provide a time constant (τ) of 211.9±12.9 ms and 155.8±19.7 ms, at 4°C and 11°C, respectively ($P<0.001$).

I_{Ca} was blocked by both CdCl$_2$ (100 μmol l^{-1}) and a combination of CdCl$_2$ (30 μmol l^{-1}) and verapamil (10 μmol l^{-1}) (see below). Isoprenaline increased peak I_{Ca} in the burbot ventricular myocytes by 65% and 95% at 4°C and 11°C, respectively (Fig. 4B,C).

The slow inactivation time constants and the long AP duration, especially at 4°C, suggest a prominent role for the I_{Ca} window current in this species. Steady-state activation and inactivation (Fig. 4D) and the I_{Ca} window current (Fig. 4E) was measured in burbot myocytes at 4°C using 5 mmol l^{-1} EGTA in the pipette. The voltage at which inactivation was half-maximal (V_h) and slope (k) that describes the Boltzman fit to inactivation are –11.95±1.37 mV and –11.14±0.89 (mean ± s.e.m., $N=9$), respectively. Corresponding values for steady-state activation are –10.89±1.20 mV and 10.40±1.43 mV, respectively. These results indicate slow transition between activation and inactivation at 4°C and result in the large window current given in Fig. 4E.

SR Ca^{2+} cycling in burbot ventricular myocytes

The Ca^{2+} stores of the burbot SR were first released with caffeine so that all myocytes started with a negligible SR Ca^{2+} content. SR Ca^{2+} was then replenished with a series of stimulus pulses which, under control conditions, consisted of 25 square pulses from –80 to +10 mV for 600 ms at a frequency of 0.2 Hz. SR Ca^{2+} accumulation was assessed by recording the NCX current generated upon the re-application of caffeine and calculating its time integral. Representative recordings of I_{NCX} and its time integral at 4°C and 11°C are given in Fig. 5A,B. The mean values for SR Ca^{2+} content in burbot myocytes at 4°C and 11°C are given in Fig. 5C and are expressed as charge (pC) normalized to myocyte capacitance (pF). The ability to load Ca^{2+} into the SR is not significantly affected by acute warming with Ca^{2+} content being 124±23 μmol l^{-1} at 4°C and 165±33 μmol l^{-1} at 11°C. This small steady-state SR Ca^{2+} content in burbot cells was not the result of incomplete Ca^{2+} release during the 3 s caffeine pulse as longer single caffeine applications of up to 10 s did not result in a greater SR Ca^{2+} release, nor did repeated shorter duration single caffeine applications (not shown).

Stimulating burbot myocytes with long square depolarizing pulses (1–4 s) to high voltages (+50 mV) did not significantly increase SR Ca^{2+} content compared with that obtained under the control loading conditions given in Fig. 5C. Furthermore, applying loading pulses (25–75 pulses, to either +10 or
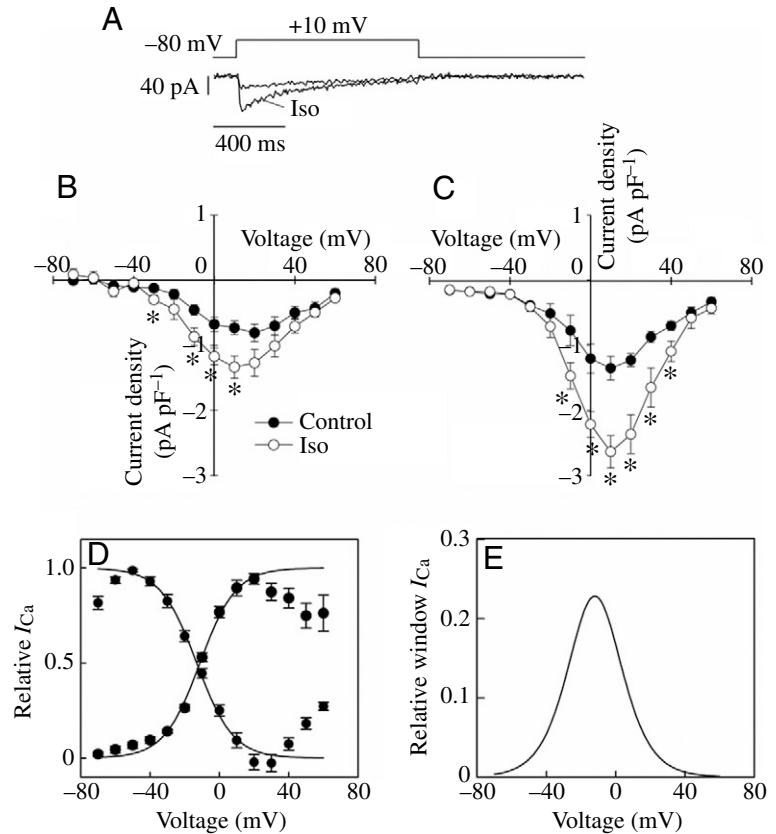
Fig. 4. L-type Ca²⁺ current in burbot ventricular myocytes measured with 5 mmol l⁻¹ EGTA in the pipette solution. (A) Representative recording at 11°C with and without stimulation by isoprenaline (10 μmol l⁻¹). Values are means ± s.e.m. from 6–12 cells at 4°C (B) and 11°C (C) under control conditions and in the presence of 10 μmol l⁻¹ isoprenaline (Iso). *Density of I_{Ca} is increased significantly by 10 μmol l⁻¹ isoprenaline (Student's *t*-test, P<0.01). (D) Steady-state activation and inactivation relationships I_{Ca} at 4°C only. (E) The I_{Ca} window current (product of activation and inactivation curves in D) at 4°C.
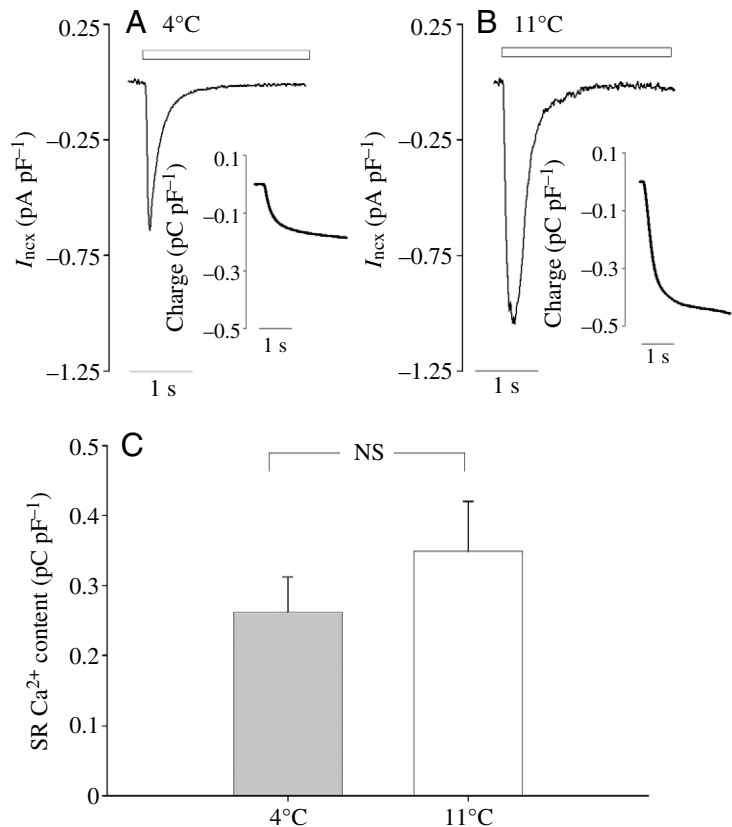
Fig. 5. SR Ca²⁺ content in burbot ventricular myocytes. Representative recordings of inward Na⁺–Ca²⁺ exchange currents (I_{NCX}) in response to caffeine (10 mmol l⁻¹, designated by the white bar) in burbot ventricular myocytes at 4°C (A) and 11°C (B). The insets show the corresponding time integral of I_{NCX} at each temperature. (C) Mean values ± s.e.m.; N=119 myocytes at 4°C and 20 myocytes at 11°C, respectively. NS, values were not significantly different (Student's *t*-test, P>0.05). SR Ca²⁺ content is expressed as the charge carried by the integral (pC) normalized to cell capacitance (pF). In the text, values for charge (pC) are converted into μmol Ca²⁺ (see Materials and methods) to facilitate comparisons with literature values.

+50 mV, for either 1 s or 4 s) in bathing solution without TTX, in an attempt to augment reverse-mode NCX, did not result in greater SR Ca^{2+} accumulation upon application of caffeine (not shown). The amount of Ca^{2+} accumulated by the SR did not significantly increase when stimulating pulses (either control pulses or 1 s pulses to +50 mV) were applied in the presence of 1 or 10 μmol l^{-1} isoprenaline, although I_{Ca} was augmented. Thus, SR Ca^{2+} content in burbot ventricular myocytes was at a steady-state between 100 and 300 μmol l^{-1} Ca^{2+} under the conditions of our study. It should be noted, however, that a few cells (11 out of 119 at 4°C and 2 out of 20 at 11°C) had an SR Ca^{2+} content in excess of 1000 μmol l^{-1} upon the first application of caffeine. Although these cells were Ca^{2+} overloaded, it does suggest that the maximal Ca^{2+} storage capacity of the burbot SR can be large.

SR Ca^{2+} levels were considerably reduced (~70%) when

control loading pulses were applied during blockade of I_{Ca} (with 100 μmol l^{-1} $CdCl_2$) or I_{NCX} (with 10 mmol l^{-1} NiCl). For example, SR Ca^{2+} content decreased from 244±72 μmol l^{-1} (*N*=13) under control conditions, to 73±20 and 75±41 μmol l^{-1} when the 25 stimulation pulses were applied in the presence of $CdCl_2$ (100 μmol l^{-1}) or $NiCl_2$ (10 mmol l^{-1}), respectively. This suggests equal SR Ca^{2+} loading capabilities of these two Ca^{2+} influx pathways. However, because $CdCl_2$ at a concentration of 100 μmol l^{-1} can potentially impact NCX activity, we examined SR Ca^{2+} accumulation in the presence of 30 μmol l^{-1} $CdCl_2$ and 10 μmol l^{-1} verapamil, which has been shown to quickly and effectively block L-type Ca^{2+} channel currents in crucian carp (*Carassius carassius*) myocytes without inhibiting the NCX (Vornanen, 1999). We found less of a reduction (~56%) in SR Ca^{2+} content under these conditions, suggesting that reverse-mode NCX contributes a greater amount of Ca^{2+} to SR stores than I_{Ca} in burbot ventricular myocytes. It is important to note that these experiments were conducted with 0.025 mmol l^{-1} EGTA in the pipette to better simulate *in vivo* cytosolic Ca^{2+} buffering (Hove-Madsen and Tort, 1998) and thus peak I_{Ca} was reduced by ~65% (to 0.28±0.02 and 0.48±0.04 pA pF^{-1} at 4°C and 11°C, respectively) compared with the values presented in Fig. 4, possibly reducing I_{Ca} contribution to SR Ca^{2+} loading. On the other hand, the lack of an increase in SR Ca^{2+} content during isoprenaline stimulation, despite augmented I_{Ca}, emphasizes the limited role of I_{Ca} and the potential importance of Ca^{2+} influx *via* NCX during excitation–contraction coupling in this species.

Inactivation kinetics of I_{Ca} were examined to assess the impact of SR Ca^{2+} release on excitation–contraction coupling in burbot myocytes at 4°C and 11°C. I_{Ca} records initiated immediately after depletion of SR Ca^{2+} by caffeine allowed the effects of subsequent progressive accumulation and release of SR Ca^{2+} on I_{Ca} to be monitored. Single exponential fits (tau, τ) to the decaying portion of I_{Ca} revealed no change in inactivation kinetics as Ca^{2+} was loaded into the SR (Fig. 6), indicating a lack of SR-Ca^{2+}-release dependent inactivation of I_{Ca} at either temperature.

Fig. 6. SR Ca^{2+} release in burbot myocytes does not affect the inactivation kinetics of I_{Ca}. Representative recordings of I_{Ca} at 4°C (A) or 11°C (B) on the first pulse after caffeine application (SR empty) and the 25th pulse after caffeine application (steady-state SR Ca^{2+} content). Recordings are superimposed. Tau of inactivation was calculated by fitting a single exponential function to the decaying portion of I_{Ca}. For clarity, only the fit for 25th pulse is shown at each temperature (red lines). (C) Values are means ± s.e.m. from 9 myocytes at 4°C and 16 myocytes at 11°C, 1, 5, 10 and 25 pulses after caffeine application. *Inactivation of I_{Ca} was faster at 11°C than at 4°C (Student's *t*-test, *P*<0.05).

Discussion

Electrophysiological properties of burbot ventricle

In general, the RMP and AP of the burbot ventricle are similar to those recorded from other vertebrate hearts (Jaeger, 1965; Anderson et al., 1977; Morad et al., 1983; Venditti et al., 1996). However, there are several features of SL ion currents in the burbot ventricle that are not especially typical for vertebrate heart. These characteristics include (i) very small I_{K1}, (ii) large I_{Kr}, (iii) small I_{Ca} and (iv) large I_{NCX}.

In cardiac myocytes, I_{K1} maintains the negative RMP and contributes to final phase 3 repolarisation (Christie, 1995; Barry and Nerbonne, 1996). I_{K1} of the burbot
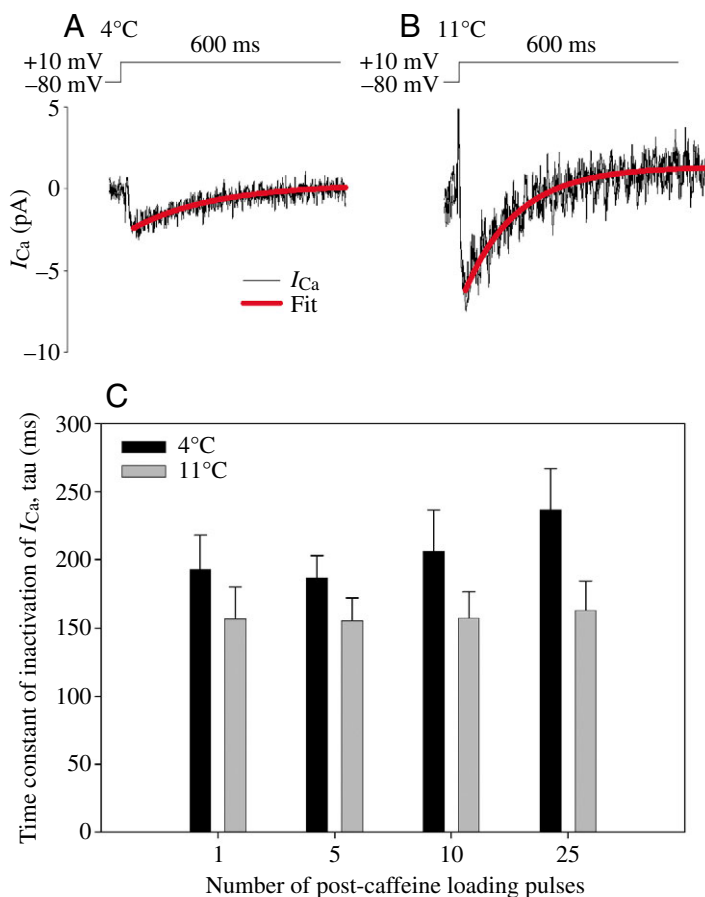
ventricle is small, only one third of those found in cold-acclimated (4°C) trout and even less than the values measured in warm-acclimated (18°C) trout and crucian carp (Paajanen and Vornanen, 2002; Paajanen and Vornanen, 2004; Vornanen et al., 2002a), which explains its 7–10 mV less negative RMP in comparison with these species. Because I_{K1} is small, it cannot contribute very much to the repolarisation of the AP. It is perhaps not unexpected then, that the other repolarising current, I_{Kr}, is about five times larger than I_{K1} in burbot ventricular myocytes. The relative sizes of K$^+$ currents in burbot ventricular myocytes resemble those of cold-acclimated trout but are in fact more extreme, with burbot ventricular K$^+$ currents showing an electrical excitability phenotype similar to atrial K$^+$ currents in other fish species (Vornanen et al., 2002a). The similarity of K$^+$ currents, i.e. small I_{K1} and large I_{Kr}, in cold-acclimated trout and burbot suggest that this might be a physiologically significant mechanism by which excitability is maintained at low temperatures. Studies on other cold-adapted species are necessary to assess the universality of this strategy and its influence on factors such as maintenance of RMP, AP duration and the prevention of cardiac arrhythmias.

Sarcolemmal Ca^{2+} transport in burbot ventricular myocytes

Fish cardiac myocytes have a large surface area-to-volume ratio, increasing the efficacy of SL ion exchange in cytosolic Ca^{2+} management. This is especially true in myocytes of the burbot heart, which are 30% smaller in both length and width than those from similarly sized rainbow trout, which should result in even smaller diffusion distances between the SL and the myofilaments (Tiitu and Vornanen, 2002a). In the physiological voltage range, the NCX avidly transports Ca^{2+} in both directions across the SL, while L-type Ca^{2+} channels provide an entry pathway for extracellular Ca^{2+} and maintain the long AP duration. The density of I_{Ca} is very low in burbot myocytes (Fig. 4) being half of that of crucian carp myocytes under identical conditions (not shown). However, the temperature sensitivity of I_{Ca} in the burbot ventricle (Q$_{10}$~2) is similar to that of other fish (Shiels et al., 2000). The low I_{Ca} density may be related to the low density of the L-type Ca^{2+} channels on the burbot SL as dihydropyridine (DHPR) binding studies have indicated significantly lower B_{max} compared with that of trout and carp (Tiitu and Vornanen, 2003). β-adrenergic stimulation increases the size of I_{Ca}, but at present the adrenergic tonus on the burbot heart and its impact on excitation–contraction coupling are unknown.

Despite the slow inactivation of I_{Ca}, the charge carried (Q_{Ca}) was still very small. Indeed, the values for Q_{Ca} after a 1 s square pulse in the burbot were similar to the values of the rainbow trout ventricular myocytes for 0.5 s pulse and 58–75% of the values of the crucian carp ventricular myocytes for 0.5 s pulse (Vornanen, 1997; Vornanen, 1998; Shiels et al., 2000) at similar temperatures and identical conditions of cytosolic Ca^{2+} buffering. Thus, I_{Ca} and Q_{Ca} in the burbot heart are smaller than in either rainbow trout or crucian carp. However, the slow inactivation of I_{Ca} may have another important role in cytosolic

Ca^{2+} management. It increases calcium influx via the I_{Ca}-window current, which may play an important role in the long APD of burbot myocytes. We have previously shown that acute cold temperature increases the I_{Ca}-window current in trout myocytes, increasing the relative importance of SL calcium influx (Shiels et al., 2000). Here we show that the size the I_{Ca} window current in burbot ventricular myocytes at 4°C is twofold greater than in rainbow trout at 7°C (Shiels et al., 2000). Despite this, the peak density of I_{Ca} is so small in the burbot that the integrated charge transfer during the duration of an AP (~1 s at 4°C) remains smaller in burbot than trout under similar experimental conditions.

I_{NCX} density in burbot ventricular myocytes is approximately double that observed in crucian carp under identical conditions (Vornanen, 1999). I_{NCX} and I_{Ca} have been measured previously in crucian carp ventricular myocytes and it was estimated they contribute almost equally to SL Ca^{2+} entry (Vornanen, 1999). The present findings show that the density of I_{NCX} is clearly larger and the density of I_{Ca} much smaller in burbot than in carp myocytes. For example, the mean current density of the I_{NCX} is 0.2615 pA pF^{-1} at +10 mV at 4°C (see Fig. 3B), and if this current is integrated for 1000 ms, it results in 0.2615 pC pF^{-1} of charge transferred in 1 s. Because only one charge is carried by the NCX for each Ca^{2+} atom, this charge density corresponds to 0.523 pC pF^{-1} if it were carried by Ca^{2+} channels. This is substantially more than that transported by L-type Ca^{2+} channels at peak current (0.24±0.043 pC pF^{-1} at the same voltage and temperature). This clearly indicates that in burbot ventricular myocytes, the NCX is much more important than L-type Ca^{2+} channels in trans-sarcolemmal Ca^{2+} influx. This is especially true when one considers that the charge transferred by the L-type Ca^{2+} channels given above was measured with 5 mmol l^{-1} EGTA in the pipette solution, which augments Ca^{2+} influx.

Studies using non-teleost expression systems demonstrate that the trout NCX temperature-sensitivity is quite low (Q$_{10}$~1.1) (Elias et al., 2001), whereas the NCX of a tropical fish species, the tilapia Oreochromis mossambicus, shows a similar temperature-sensitivity to mammals (Marshall et al., 2005). Surprisingly, the burbot I_{NCX} shows a relatively strong temperature dependence (Q$_{10}$=2.47) between 4°C and 11°C when recorded in native myocytes. This is interesting in light of the cold stenothermic environment in which the burbot lives and the predominance of the NCX in mediating SL Ca^{2+} flux. It should be noted, however, that regardless of the Q$_{10}$-effect, the activity of the NCX at 4°C is still high in burbot in comparison with other fish species. Further studies are necessary to assess the impact of this temperature sensitivity on excitation–contraction coupling.

SR Ca^{2+} cycling in burbot ventricular myocytes

We found the SR Ca^{2+} content in burbot ventricular myocytes was at a steady state between 100 and 300 μmol l^{-1}, which is comparable to that observed in mammals [100–150 μmol l^{-1} (Bassani et al., 1995; Negretti et al., 1995)] but smaller than that reported for rainbow trout myocytes

(>500 μmol l^{-1}) (Hove-Madsen et al., 1998; Shiels et al., 2002b).

In the present study we examined the effect of SR Ca^{2+} content on the inactivation kinetics of I_{Ca} as an indirect means of assessing Ca^{2+}-induced Ca^{2+}-release (CICR). Despite the modest total SR Ca^{2+} content, we had expected to see evidence of CICR in burbot myocytes given that (i) isolated muscle experiments show that SR Ca^{2+} contributes significantly to contractility (Tiitu and Vornanen, 2002b), (ii) electron micrographs of burbot ventricle show that peripheral couplings between the SR and the SL are bridged by distinct foot particles akin to ryanodine receptors, indicating the structural organization necessary for CICR (Tiitu and Vornanen, 2002a), and (iii) [^{3}H]ryanodine binding studies in cardiac vesicles indicate that the burbot ventricle has a substantial number of ryanodine receptors (65% of the value of the rat heart) whose opening is very Ca^{2+} sensitive (Vornanen, 2006). However, we saw no effect of SR Ca^{2+} content on the inactivation kinetics of I_{Ca}, which suggests limited CICR in burbot ventricular myocytes. This apparent contradiction may be related to the low density of the L-type Ca^{2+} channels, which may preclude sufficient trigger signal for propagative CICR (see Shiels and White, 2005). Alternatively, as the NCX can provide the trigger Ca^{2+} in both mammal and fish hearts (Vornanen et al., 1994; Hove-Madsen et al., 2003), it is possible that the large I_{NCX} of the burbot ventricular myocytes overwhelms I_{Ca} as a trigger in the dyadic junction and, at the same time, masks the effect of CICR on I_{Ca} inactivation. According to this proposal the relative roles of I_{Ca} and I_{NCX} in triggering SR Ca^{2+} release would be quite different in fish and mammalian hearts. Obviously further studies examining the time course of intracellular Ca^{2+} transients in burbot ventricle with and without SR inhibition would provide valuable insight into the physiological role and mechanism of SR Ca^{2+} cycling during excitation–contraction coupling in this species.

Conclusions

Electrical excitation of burbot ventricular myocytes suggest that cold stenothermy and compensatory cold-acclimation involve many of the same subcellular mechanisms. In particular, burbot K$^+$ currents are organised similarly to those of cold-acclimated active species, demonstrating a small delayed rectifier K$^+$ current (I_{Kr}) and a large inward rectifier K$^+$ current (I_{K1}). This data strongly suggests that K$^+$ current re-organisation may be necessary for AP regulation in cold-adapted species. Based on inactivation of I_{Ca}, we found no evidence of an upregulation of SR Ca^{2+} flux pathways in burbot ventricular myocytes, which is contrary to previous findings from other cold-acclimated fish. This may be related to the fluminous Ca^{2+} influx through the NCX, which probably provides the major part of the contractile Ca^{2+}.

List of abbreviations

AP	action potential
APD	action potential duration
CICR	Ca^{2+}-induced Ca^{2+}-release
NCX	Na^{2+}–Ca^{2+} exchange
RMP	resting membrane potential
SL	sarcolemma
SR	sarcoplasmic reticulum

References

Aho, E. and Vornanen, M. (1999). Contractile properties of atrial and ventricular myocardium of the heart of rainbow trout (*Oncorhynchus mykiss*): effects of thermal acclimation. *J. Exp. Biol.* **202**, 2663-2677.

Anderson, T. W., Hirsch, C. and Kavaler, F. (1977). Mechanism of activation of contraction in frog ventricular muscle. *Circ. Res.* **41**, 472-480.

Barry, D. M. and Nerbonne, J. M. (1996). Myocardial potassium channels: electrophysiological and molecular diversity. *Annu. Rev. Physiol.* **58**, 363-394.

Bassani, J. W., Yuan, W. and Bers, D. M. (1995). Fractional SR Ca release is regulated by trigger Ca and SR Ca content in cardiac myocytes. *Am. J. Physiol.* **268**, C1313-C1319.

Bowler, K. and Tirri, R. (1990). Temperature dependence of the heart isolated from the cold or warm acclimated perch (*Perca fluviatilis*). *Comp. Biochem. Physiol.* **96A**, 177-180.

Carl, L. (1995). Sonic tracking of Burbot in Lake Openongo, Ontario. *Trans. Am. Fish. Soc.* **124**, 77-83.

Christie, M. J. (1995). Molecular and functional diversity of K$^+$ channels. *Clin. Exp. Pharmacol. Physiol.* **22**, 944-951.

Driedzic, W. R. and Gesser, H. (1994). Energy-metabolism and contractility in ectothermic vertebrate hearts: hypoxia, acidosis, and low-temperature. *Physiol. Rev.* **74**, 221-258.

Elias, C. L., Xue, X. H., Marshall, C. R., Omelchenko, A., Hryshko, L. V. and Tibbits, G. F. (2001). Temperature dependence of cloned mammalian and salmonid cardiac Na$^+$/Ca^{2+} exchanger isoforms. *Am. J. Physiol.* **281**, C993-1000.

Gillis, T. E. and Tibbits, G. F. (2002). Beating the cold: the functional evolution of troponin C in teleost fish. *Comp. Biochem. Physiol.* **132A**, 763-772.

Gillis, T. E., Marshall, C. R., Xue, X. H., Borgford, T. J. and Tibbits, G. F. (2000). Ca^{2+} binding to cardiac troponin C: effects of temperature and pH on mammalian and salmonid isoforms. *Am. J. Physiol.* **279**, R1707-R1715.

Gillis, T. E., Moyes, C. D. and Tibbits, G. F. (2003). Sequence mutations in teleost cardiac troponin C that are permissive of high Ca^{2+} affinity of site II. *Am. J. Physiol.* **284**, C1176-C1184.

Goolish, E. (1987). Cold acclimation increases the ventricle size of carp, *Cyprinus carpio*. *J. Therm. Biol.* **12**, 203-205.

Graham, M. S. and Farrell, A. P. (1989). The effect of temperature-acclimation and adrenaline on the performance of a perfused trout heart. *Physiol. Zool.* **62**, 38-61.

Harwood, C. L., Howarth, F. C., Altringham, J. D. and White, E. (2000). Rate-dependent changes in cell shortening; intracellular Ca^{2+} levels and membrane potential in single isolated rainbow trout (*Oncorhynchus mykiss*) ventricular myocytes. *J. Exp. Biol.* **203**, 493-504.

Hove-Madsen, L. and Tort, L. (1998). L-type Ca^{2+} current and excitation-contraction coupling in single atrial myocytes from rainbow trout. *Am. J. Physiol.* **275**, R2061-R2069.

Hove-Madsen, L., Llach, A. and Tort, L. (1998). Quantification of Ca^{2+} uptake in the sarcoplasmic reticulum of trout ventricular myocytes. *Am. J. Physiol.* **44**, R2070-R2080.

Hove-Madsen, L., Llach, A., Tibbits, G. F. and Tort, L. (2003). Triggering of sarcoplasmic reticulum Ca^{2+} release and contraction by reverse mode Na$^+$/Ca^{2+} exchange in trout atrial myocytes. *Am. J. Physiol.* **284**, R1330-R1339.

Jaeger, R. (1965). Aktionpotentiale der myokardfasern des fischherzens. *Naturwissenschaften* **52**, 482-483.

Keen, J. E., Vianzon, D. M., Farrell, A. P. and Tibbits, G. F. (1994). Effect

of temperature and temperature-acclimation on the ryanodine sensitivity of the trout myocardium. *J. Comp. Physiol. B* **164**, 438-443.

Marshall, C. R., Pan, T. C., Le, H. D., Omelchenko, A., Hwang, P. P., Hryshko, L. V. and Tibbits, G. F. (2005). cDNA cloning and expression of the cardiac Na$^+$/Ca^{2+} exchanger from Mozambique tilapia (*Oreochromis mossambicus*) reveal a teleost membrane transporter with mammalian temperature dependence. *J. Biol. Chem.* **280**, 28903-28911.

Morad, M., Goldman, Y. E. and Trentham, D. R. (1983). Rapid photochemical inactivation of Ca^{2+}-antagonists shows that Ca^{2+} entry directly activates contraction in frog heart. *Nature* **304**, 635-638.

Negretti, N., Varro, A. and Eisner, D. A. (1995). Estimate of net calcium fluxes and sarcoplasmic reticulum calcium content during systole in rat ventricular myocytes. *J. Physiol.* **486**, 581-591.

Paajanen, V. and Vornanen, M. (2002). The induction of an ATP-sensitive K$^+$ current in cardiac myocytes of air- and water-breathing vertebrates. *Pflugers Arch.* **444**, 760-770.

Paajanen, V. and Vornanen, M. (2004). Regulation of action potential duration under acute heat stress by I$_{(K,ATP)}$ and I$_{(K1)}$ in fish cardiac myocytes. *Am. J. Physiol.* **286**, R405-R415.

Pääkkönen, J.-P. and Marjomäki, T. J. (2000). Feeding of burbot, *Lota lota*, at different temperatures. *Environ. Biol. Fishes* **58**, 109-112.

Shiels, H. A. and Farrell, A. P. (1997). The effect of temperature and adrenaline on the relative importance of the sarcoplasmic reticulum in contributing Ca^{2+} to force development in isolated ventricular trabeculae from rainbow trout. *J. Exp. Biol.* **200**, 1607-1621.

Shiels, H. A. and White, E. (2005). Temporal and spatial properties of cellular Ca^{2+} flux in trout ventricular myocytes. *Am. J. Physiol.* **288**, R1756-R1766.

Shiels, H. A., Vornanen, M. and Farrell, A. P. (2000). Temperature-dependence of L-type Ca^{2+} channel current in atrial myocytes from rainbow trout. *J. Exp. Biol.* **203**, 2771-2780.

Shiels, H. A., Vornanen, M. and Farrell, A. P. (2002a). Effects of temperature on intracellular [Ca^{2+}] in trout atrial myocytes. *J. Exp. Biol.* **205**, 3641-3650.

Shiels, H. A., Vornanen, M. and Farrell, A. P. (2002b). Temperature dependence of cardiac sarcoplasmic reticulum function in rainbow trout myocytes. *J. Exp. Biol.* **205**, 3631-3639.

Tiitu, V. and Vornanen, M. (2002a). Morphology and fine structure of the heart of the burbot (*Lota lota*), a cold stenothermal fish. *J. Fish Biol.* **61**, 106-121.

Tiitu, V. and Vornanen, M. (2002b). Regulation of cardiac contractility in a stenothermal fish, the burbot (*Lota lota*). *J. Exp. Biol.* **205**, 1597-1606.

Tiitu, V. and Vornanen, M. (2003). Ryanodine and dihydropyridine receptor binding in ventricular cardiac muscle of fish with different temperature preferences. *J. Comp. Physiol. B* **173**, 285-291.

Varro, A., Negretti, N., Hester, S. B. and Eisner, D. A. (1993). An estimate of the calcium content of the sarcoplasmic reticulum in rat ventricular myocytes. *Pflügers Arch.* **423**, 158-160.

Venditti, P., Di Meo, S., de Martino Rosaroll, P. and De Leo, T. (1996). Effect of T$_3$ administration on electrophysiological properties of lizard ventricular muscle fibres. *J. Comp. Physiol. B* **165**, 552-557.

Vornanen, M. (1996). Effect of extracellular calcium on the contractility of warm- and cold-acclimated crucian carp heart. *J. Comp. Physiol. B* **165**, 507-517.

Vornanen, M. (1997). Sarcolemmal Ca influx through L-type Ca channels in ventricular myocytes of a teleost fish. *Am. J. Physiol.* **41**, R1432-R1440.

Vornanen, M. (1998). L-type Ca^{2+} current in fish cardiac myocytes: effects of thermal acclimation and beta-adrenergic stimulation. *J. Exp. Biol.* **201**, 533-547.

Vornanen, M. (1999). Na$^+$/Ca^{2+} exchange current in ventricular myocytes of fish heart: contribution to sarcolemmal Ca^{2+} influx. *J. Exp. Biol.* **202**, 1763-1775.

Vornanen, M. (2006). Temperature- and Ca^{2+}-dependence of [^{3}H]ryanodine binding in the burbot (*Lota lota* L.) heart. *Am. J. Physiol.* **290**, R345-R351.

Vornanen, M., Shepherd, N. and Isenberg, G. (1994). Tension-voltage relations of single myocytes reflect Ca^{2+} release triggered by Na$^+$/Ca^{2+} exchange at 35°C but not 23°C. *Am. J. Physiol.* **267**, C623-C632.

Vornanen, M., Ryökkynen, A. and Nurmi, A. (2002a). Temperature-dependent expression of sarcolemmal K$^+$ currents in rainbow trout atrial and ventricular myocytes. *Am. J. Physiol.* **282**, R1191-R1199.

Vornanen, M., Shiels, H. A. and Farrell, A. P. (2002b). Plasticity of excitation-contraction coupling in fish cardiac myocytes. *Comp. Biochem. Physiol.* **132A**, 827-846.

Yang, H., Velema, J., Hedrick, M. S., Tibbits, G. F. and Moyes, C. D. (2000). Evolutionary and physiological variation in cardiac troponin C in relation to thermal strategies of fish. *Physiol. Biochem. Zool.* **73**, 841-849.